Heliyon 9 (2023) e18156

Contents lists available at ScienceDirect

Heliyon

journal homepage: www.cell.com/heliyon

Investigation of mode coupling in strained and unstrained multimode step-index POFs using the Langevin equation

Svetislav Savović [a], Konstantinos Aidinis [b,c], Alexandar Djordjevich [d], Rui Min [e,*]

[a] University of Kragujevac, R. Domanovića 12, 34000, Kragujevac, Serbia
[b] Department of Electrical Engineering, Ajman University, P.O. Box 346, Ajman, United Arab Emirates
[c] Center of Medical and Bio-allied Health Sciences Research, Ajman University, P. O. Box 346, Ajman, United Arab Emirates
[d] City University of Hong Kong, 83 Tat Chee Avenue, Kowloon, China
[e] Center for Cognition and Neuroergonomics, State Key Laboratory of Cognitive Neuroscience and Learning, Beijing Normal University, Zhuhai, 519087, China

ARTICLE INFO

Keywords:
Polymer optical fibers
Langevin equation
Mode coupling
Coupling length

ABSTRACT

The Langevin equation (LE) is used to evaluate mode coupling in multimode step-index polymer optical fiber (SI POF) that is both unstrained and strained. The numerical solution of the LE matches the numerical solution of the power flow equation (PFE). Strain-induced mode coupling is noticeably stronger in strained fiber than in unstrained fiber of the same types. Therefore, compared to similar lengths for unstrained fibers, the coupling length of the equilibrium mode distribution (EMD) is attained and the length of fiber required to produce a steady-state distribution (SSD) are both much shorter for strained fibers. We have demonstrated that the mode coupling in strained and unstrained multimode SI POFs that comes from the random perturbations (RPs) of the fiber can be successfully treated by the LE. The study's findings can be used to improve communication and sensory systems that use multimode SI POFs under different bending circumstances. Additionally, it is crucial to be able to compute the modal distribution of the SI POFs used in the optical fiber sensory system at a specific length and under various bending scenarios.

1. Introduction

The preferred transmission medium in long-distance communication systems for decades has been silica optical fibers [1,2]. A multimode POF, on the other hand, is often considered for high-performance short data lines (less than 100 m) [3,4]. Since POFs pair light effectively because of their wide diameter and high NA, many POF applications in power delivery systems [5,6], sensors [7,8], and short-range communication links [9,10] have been investigated. Applications for POF have a market with room for expansion in huge, complex constructions, moving vehicles, or locations where the network is periodically rebuilt [11,12].

Intrinsic fiber's RP effects, such as minute bends, abnormalities at the core and cladding interface, and modifications in the refractive index (RI) distribution, are the cause of mode coupling. In practice, RPs in POFs are realized by heating, bending, radiating, corrugating and etching. Mode coupling improves bandwidth and reduces modal dispersion [13]. For example, a stronger mode coupling can be achieved by using a mode scrambler near the input fiber end [14]. The output field pattern would vary with fiber

* Corresponding author.
E-mail address: rumi@doctor.upv.es (R. Min).

https://doi.org/10.1016/j.heliyon.2023.e18156
Received 27 February 2023; Received in revised form 7 July 2023; Accepted 10 July 2023
Available online 17 July 2023

length from the one that was initially provided at the input fiber end until EMD was achieved. Mode coupling in optical fibers has been the subject of much theoretical and practical study as a result of these features. It has been studied using the PFE for different launching conditions and NA [14–18]. Mode coupling has been observed to increase as a result of bending strain [19,20]. We refer to the POFs in this study as "strained POFs" and compare their behavior to that of "unstrained POFs" because significant long-duration bending has changed the coupling properties. We describe how mode coupling in both strained and unstrained SI POFs was successfully addressed using the LE [21]. The mathematical formulation of the stochastic mode coupling problem is provided by the LE.

2. The PFE and the Fokker-Planck equation

The Gloge's time-independent PFE is shown as below [15]:

$$\frac{\partial P(\theta,z)}{\partial z} = -\alpha(\theta)P(\theta,z) + \frac{D}{\theta}\frac{\partial}{\partial\theta}\left(\theta\frac{\partial P(\theta,z)}{\partial\theta}\right) \tag{1}$$

where $P(\theta,z)$ is the angular power distribution, θ is the propagation angle, z is the light traveling distance along the fiber, D is the constant coupling coefficient [14–18] and $\alpha(\theta)$ is the modal attenuation. Due to $\alpha(\theta)$ is negligible when $\theta \approx \theta_c$, equation (1) becomes the following diffusion equation [18]:

$$\frac{\partial P(\theta,z)}{\partial z} = \frac{D}{\theta}\frac{\partial P(\theta,z)}{\partial\theta} + D\frac{\partial^2 P(\theta,z)}{\partial\theta^2} \tag{2}$$

Thus, the internal energy redistribution process of the multimode optical fiber resembles diffusion. The solutions to stochastic differential equations (SDEs) represent systems with RPs and function as models for diffusion, as is well known [21]. As mode coupling in multimode optical fibers occurs from inherent RPs, an SDE could be used to explain it. To do this, equation (2) is approximately represented as:

$$\frac{\partial P(\theta,z)}{\partial z} = -V\frac{\partial P(\theta,z)}{\partial\theta} + D\frac{\partial^2 P(\theta,z)}{\partial\theta^2} \tag{3}$$

where V is constant drift coefficient [14,16–18]. If consider $P(\theta,z)$ as a probability distribution, equation (3) is therefore revealed to be the Fokker-Planck equation (FPE) [21]. The drift coefficient V is given as:

$$V = (1/M)\sum_{r=1}^{M} V_r \tag{4}$$

In equation (4), V_r is the r-th's mode drift coefficient.

3. The Langevin equation

The FPE (3) transformed into the following form of the LE [21]:

$$\frac{\mathrm{d}\theta}{\mathrm{d}z} = h + g\Gamma(z) \tag{5}$$

where $g\Gamma(z)$ is the Gaussian distributed random Langevin force with the strength g. Equation (5) is SDE due to it contains the random force, such that we have [9]:

$$\begin{aligned}\langle\Gamma(z)\rangle &= 0\\ \langle\Gamma(z)\Gamma(z')\rangle &= 2\delta(z-z')\end{aligned} \tag{6}$$

Using equation (6) and adhering to the Ito rule [21], one gets $V=h$ and $D=g^2$. Finally, the LE is given as:

$$\frac{d\theta}{dz} = V + \sqrt{D}\Gamma(z) \tag{7}$$

The first term on the right-hand side of (7) has behavior that is entirely deterministic. The distribution is shifted in the direction of $= 0$ as a result. The impacts of the stochastic nature and internal noise of the fiber's intrinsic perturbations are shown in the second term. It is describes broadening the θ distribution. It should be observed that when the boundary condition in equation (7) is satisfied, equation (7) reduces to equation (8), when the boundary condition in equation (2) $D(\partial P/\partial\theta)$=0 at $\theta = 0$ is satisfied:

$$\frac{d\theta}{dz} = \sqrt{D}\Gamma(z) \tag{8}$$

The angle θ_{n+1} at optical fiber length z_{n+1} could be determined by solving the LE (7), which is re-written as:

$$\theta_{n+1} = \theta_n + Vk + \sqrt{Dk}\omega_n \tag{9}$$

where $n=0, \ldots, N$-1 and $\omega_0, \ldots, \omega_{N-1}$ are independent Gaussian random numbers such that $<\omega_n>= 0$ and $<\omega_n\omega_{n'}>= 2\delta_{nm}$.

According to equation (8), equation (9) for $\theta_n = 0$, becomes:

$$\theta_{n+1} = \sqrt{Dk}\omega_n \tag{10}$$

Thus, one obtains $\theta_N = \theta(z_f)$. By computing a large number of representations of ω_n, and average them over intervals $\Delta\theta$ for $0 \leq \theta \leq \theta_c$, one obtains $< \theta(z_f) >$. It is important to note that optical fiber perturbations are known to be random. In contrast to the deterministic PFE (2) and FPE (3), the LE explicitly describes the stochastic process of energy redistribution in optical fiber. In this work, in our knowledge for the first time, a mode coupling process in strained POFs is investigated using the LE.

4. Numerical results and discussion

Here, we investigated the multimode SI POF that was experimentally tested by Losada et al. [19] under both strained and unstrained conditions. This POF was from Toray: PFU-CD1001-22E (PFU), and it had a 1-mm-diameter polymethylmethacrylate core, numerical aperture NA = 0.46, and RI of the core $n_1 = 1.492$. The number of modes that propagate along this fiber at $\lambda = 633$ nm is: $N = 2\pi^2 a^2 (NA)^2/\lambda^2 \approx 2.6 \times 10^6$. This large number of modes, which is required for the adoption of the approach proposed in this paper, may be represented by a modal continuum.

Parts of the POF were bent at regular intervals to produce consistent bending strain, as illustrated in Fig. 1, and their mode coupling characteristics were assessed while other segments were kept unaltered for comparison [19]. Coupling coefficient values $D = 7.3 \times 10^{-4}$ rad^2/m for the unstrained and $D = 1.3 \times 10^{-2}$ rad^2/m for the strained PFU POF, have been previously reported [19] – which have been adopted in this work. For the explicit finite-difference (EFD) approach to be stable, step lengths of $\Delta\theta = 0.05^\circ$ and $\Delta z = 0.0002$ m were utilized to solve the PFE (2). With a constant step-length $k = 0.0005$ m, the LE is solved using Monte-Carlo sampling of 5×10^5 representations of the ω_n in equations (9) and (10) in the intervals of $\Delta\theta = 0.05^\circ$.

Figs. 2 and 3 depict the power distribution for different POF lengths as calculated numerically using the LE (5) and the PFE (2) for unstrained PFU POF. From Figs. 4 and 5, one can compare the power distribution for varied POF lengths as determined by the solutions of the LE (5) and the PFE (2) for strained PFU POF, respectively. We present results for launch angles $\theta_0 = 0, 5, 10,$ and 15°. The numerical solutions of the LE and PFE can be seen to be in good agreement. For short POF shown in Fig. 2(a) and 3(a) 4(a) and 5(a), low-order modes' distributions have shifted towards $\theta = 0^\circ$. Longer POF lengths allow for the coupling of higher-order modes as Fig. 2 (b), 3(b) and 4(b) and 5(b) shown. For the unstrained PFU POF, the EMD is achieved at coupling length $L_c = 18$ m, where the highest-order modes shift their distribution to $\theta = 0^\circ$ as Fig. 2(c) and 3(c) shown. Fig. 4(c) and 5(c) indicate that coupling length of $L_c = 0.9$ m characterizes the strained PFU POF. The SSD is reached at length $z_s = 49$ m in Fig. 2(d) and 3(d) for the unstrained PFU POF and in Fig. 4(d) and 5(d) at length $z_s = 2.5$ m for the strained PFU POF. The coupling coefficient D for strained POFs is more than an order of magnitude larger than for an unstrained POF. This leads to much shorter characteristic lengths L_c and z_s for equivalent strained POFs.

It should be noted that we have determined the drift coefficients V=(–0.291 ± 0.005) and (−0.015 ± 0.005) rad/m for the strained and unstrained PFU POF, respectively, by averaging V_r ($r = 1, 2, 3$) for modes with launch angles $\theta_0 = 5, 10$ and 15° in equation (4).

The LE does not have the same issue as the FPE and PFE, which require a very fine mesh in the FD approach to get highly accurate numerical solution (high memory consumption). Speed of execution, memory consumption and complexity are used to measure the effectiveness of the LE integration algorithm and the EFD algorithm for obtaining the numerical solution of the PFE. Execution times for the LE and the PFE on the Intel(R) Core(TM) i3 CPU 540 @ 3.07 GHz computer for the longest investigated fiber length of 49 m are 1.2 min and 1.7 min, respectively. When expressed in terms of a 2-dim array, the memory requirements for the LE and the PFE are 656 × 3.1 × 105 and 656 × 3.1 × 106, respectively. Compared to the solution of the LE, the EFD solution of the PFE is more difficult.

To summarize, we have shown that the LE can be used to effectively treat a light transmission in multimode SI POFs that are both strained and unstrained. Unlike to the FPE and the PFE, the stability of the numerical solutions for the LE does not require special consideration. The results of this study can be used to predict the signal transmission performance of strained and unstrained SI POFs in communication or sensing systems [22,23]. For instance, varying bending circumstances result in varying fiber strain, varying mode coupling coefficient D, and subsequently varying modal distribution. Utilizing a POF as a strain sensor is possible using this POF feature. A similar approach has been used in investigation of mode coupling in unaltered low NA POFs [24] and microstructured POFs [25].

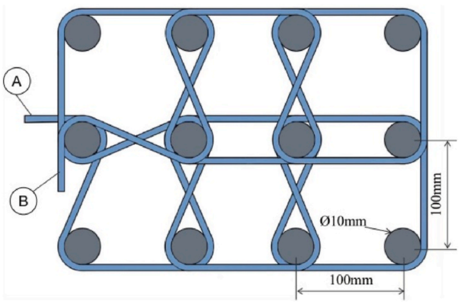

Fig. 1. An illustration of the experimental setup for creating bending strain [7].

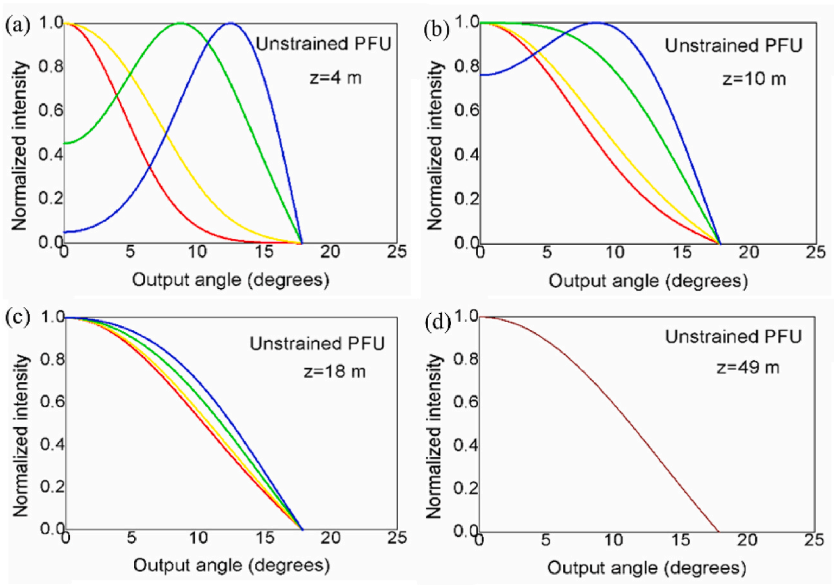

Fig. 2. Power distribution normalized at various points along the unstrained PFU POF calculated by solving the LE (5) for four Gaussian input angles $\theta_0 = 0^\circ$ (red line), 5° (yellow line), 10° (green line) and 15° (blue line) for: (a) $z = 4$ m; (b) $z = 10$ m; (c) $z = 18$ m and (d) $z = 49$ m.

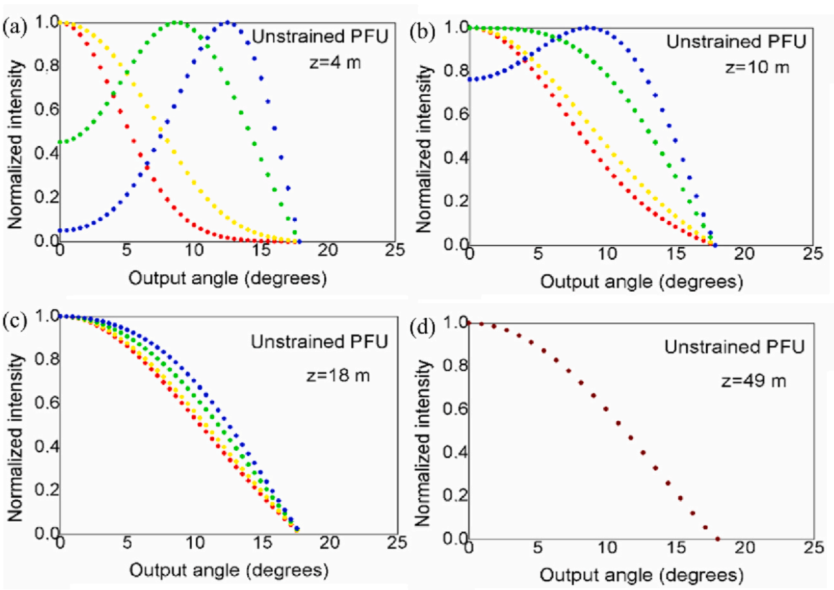

Fig. 3. Power distribution normalized at various points along the unstrained PFU POF calculated by solving the PFE (2) for four Gaussian input angles $\theta_0 = 0^\circ$ (red dots), 5° (yellow dots), 10° (green dots) and 15° (blue dots) for: (a) $z = 4$ m; (b) $z = 10$ m; (c) $z = 18$ m and (d) $z = 49$ m.

5. Conclusions

In this paper, we investigated a transmission properties of strained and unstrained multimode SI POFs using the LE. When compared to unstrained POF of the same type, strained POF exhibits substantially stronger mode coupling. As a result, strained POFs have much shorter coupling lengths than unstrained POFs and require a shorter POF length to form an SSD. The LE explicitly recognizes the stochastic nature of the various inherent perturbation strengths of the strained and unstrained SI POFs. We have demonstrated that a mode coupling process in multimode SI POFs, both strained and unstrained, may be successfully addressed by the LE. The results of this study can be applied to sensory and communication systems that employ multimode SI POFs at various bending conditions.

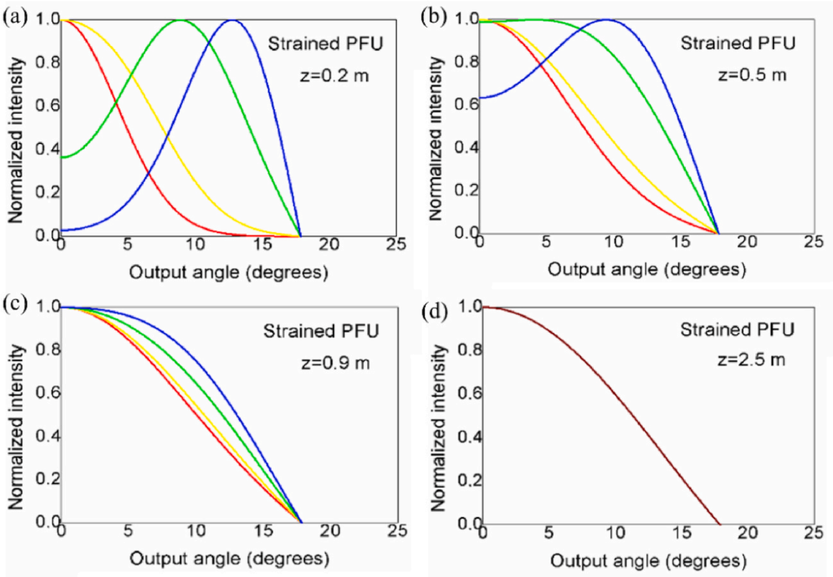

Fig. 4. Power distribution normalized at various points along the strained PFU POF calculated by solving the LE (5) for four Gaussian input angles $\theta_0 = 0^\circ$ (red line), 5° (yellow line), 10° (green line) and 15° (blue line) for: (a) $z = 0.2$ m; (b) $z = 0.5$ m; (c) $z = 0.9$ m and (d) $z = 2.5$ m.

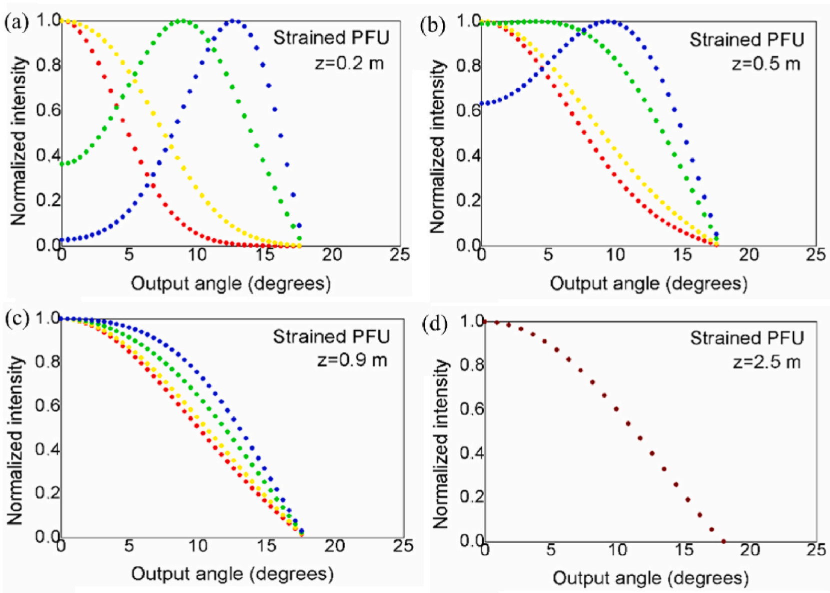

Fig. 5. Power distribution normalized at various points along the strained PFU POF was calculated by solving the PFE (2) for four Gaussian input angles $\theta_0 = 0^\circ$ (red dots), 5° (yellow dots), 10° (green dots), and 15° (blue dots) for: (a) $z = 0.2$ m; (b) $z = 0.5$ m; (c) $z = 0.9$ m and (d) $z = 2.5$ m

Funding statement

This research was funded by National Natural Science Foundation of China (62111530238, 62003046); Serbian Ministry of Education, Science and Technological Development grant (451-03-47/2023-01/200122); Science Fund of the Republic of Serbia (CTPCF-6379382); Strategic Research Grant of City University of Hong Kong (CityU 7004600); Guangdong Provincial Department of Science and Technology (2021A1313030055); The Innovation Team Project of Guangdong Provincial Department of Education (2021KCXTD014); Special project in key field of Guangdong Provincial Department of Education (2021ZDZX1050); Guangdong Basic and Applied Basic Research Foundation (2021A1515011997).

Data availability statement

Data will be made available on request.

Additional information

No additional information is available for this paper.

Author contribution statement

Svetislav Savović: Conceived and designed the experiments; Performed the experiments; Analyzed and interpreted the data; Contributed reagents, materials, analysis tools or data; Wrote the paper.

Konstantinos Aidinis, Alexandar Djordjevich, and Rui Min: Analyzed and interpreted the data; Contributed reagents, materials, analysis tools or data; Wrote the paper.

Declaration of competing interest

The authors declare that they have no known competing financial interests or personal relationships that could have appeared to influence the work reported in this paper.

References

[1] B.J. Puttnam, R. Georg, L. Ruben, Space-division multiplexing for optical fiber communications, Optica 8 (9) (2021) 1186–1203.
[2] R. Min, Z. Liu, L. Pereira, C. Yang, Q. Sui, C. Marques, Optical fiber sensing for marine environment and marine structural health monitoring: a review, Opt Laser. Technol. 140 (2021), 107082.
[3] C.R.B. Correa, F.M. Huijskens, E. Tangdiongga, A.M.J. Koonen, Luminaire-free gigabits per second LiFi transmission employing WDM-over-POF, in: The 46th European Conference on Optical Communications, ECOC), 2020, pp. 1–4.
[4] A. Inoue, Y. Koike, Unconventional plastic optical fiber design for very short multimode fiber link, Opt Express 27 (9) (2019) 12061–12069.
[5] C. Vázquez, J.D. López-Cardona, D.S. Montero, I. Pérez, P.C. Lallana, F.M. Al-Zubaidi, Power over fiber in radio over fiber systems in 5G scenarios, The 21st international conference on transparent optical networks (ICTON) (2019) 1–4.
[6] A. Fahad Ma, D.S. Montero, C. Vázquez, SI-POF supporting power-over-fiber in multi-Gbit/s transmission for in-home networks, J. Lightwave Technol. 39 (1) (2021) 112–121.
[7] R. He, C. Teng, S. Kumar, C. Marques, R. Min, Polymer optical fiber liquid level sensor: a review, IEEE Sensor. J. 22 (2) (2021) 1081–1091.
[8] R. Kuang, Y. Ye, Z. Chen, R. He, I. Savović, A. Djordjevich, S. Savovic, B. Ortega, C. Marques, X. Li, R. Min, Low-cost plastic optical fiber integrated with smartphone for human physiological monitoring, Opt. Fiber Technol. 71 (2022), 102947.
[9] O. Huang, J. Shi, N. Chi, Performance and complexity study of a neural network post-equalizer in a 638-nm laser transmission system through over 100-m plastic optical fiber, Opt. Eng. 61 (12) (2022), 126108.
[10] J.A. Apolo, B. Ortega, V. Almenar, Hybrid POF/VLC links based on a single LED for indoor communications, Photonics 8 (7) (2021) 254.
[11] D. Fujimoto, H.H. Lu, K. Kumamoto, S.E. Tsai, Q.P. Huang, J.Y. Xie, Phase-modulated hybrid high-speed Internet/WiFi/Pre-5G in-building networks over SMF and PCF with GI-POF/IVLLC transport, IEEE Access 7 (2019) 90620–90629.
[12] O. Sugihara, Gigabit and multi-gigabit data transmission for next-generation automotive optical network, The 24th OptoElectronics and Communications Conference (OECC) (2019) 1–3.
[13] M.Á. Losada, M. Mazo, A. López, C. Muzás, J. Mateo, Experimental assessment of the transmission performance of step index polymer optical fibers using a green laser diode, Polymers 13 (2021) 3397.
[14] S. Savović, A. Djordjevich, Influence of numerical aperture on mode coupling in step-index plastic optical fibers, Appl. Opt. 43 (2004) 5542–5546.
[15] D. Gloge, Optical power flow in multimode fibers, Bell Syst. Tech. J. 51 (1972) 1767–1783.
[16] W.A. Gambling, D.N. Payne, H. Matsumura, Mode conversion coefficients in optical fibers, Appl. Opt. 14 (1975) 1538–1542.
[17] M. Rousseau, L. Jeunhomme, Numerical solution of the coupled-power equation in step index optical fibers, IEEE Trans. Microw. Theor. Tech. 25 (1977) 577–585.
[18] A. Djordjevich, S. Savović, Investigation of mode coupling in step index plastic optical fibers using the power flow equation, IEEE Photon. Technol. Lett. 12 (2000) 1489–1491.
[19] M.A. Losada, J. Mateo, I. Garcés, J. Zubía, J.A. Casao, P. Peréz-Vela, Analysis of strained plastic optical fibers, IEEE Photon. Technol. Lett. 16 (2004) 1513–1515.
[20] S. Savović, M.S. Kovačević, A. Djordjevich, J.S. Bajić, D.Z. Stupar, G. Stepniak, Mode coupling in low NA plastic optical fibers, Opt Laser. Technol. 60 (2014) 85–89.
[21] H. Risken, The Fokker-Planck Equation, Springer-Verlag, Berlin, 1989.
[22] O. Ziemann, J. Krauser, P.E. Zamzow, W. Daum, POF Handbook - Optical Short Range Transmission Systems, Springer-Verlag, Berlin, 2008.
[23] M. Szczerska, Temperature sensors based on polymer fiber optic interferometer, Chemosensors 10 (2022) 228.
[24] S. Savović, A. Djordjevich, Investigation of mode coupling in low and high NA step index plastic optical fibers using the Langevin equation, J. Mod. Opt. 67 (2020) 958–962.
[25] S. Savović, L. Li, I. Savović, A. Djordjevich, R. Min, Treatment of mode coupling in step-index multimode microstructured polymer optical fibers by the Langevin equation, Polymers 14 (2022) 1243.